ELSEVIER

www.elsevier.nl/locate/jorganchem

Journal of Organometallic Chemistry 592 (1999) 296–305

Journal of Organometallic Chemistry

Synthesis, spectroscopic and structural characterisation of chromium(0), molybdenum(0) and tungsten(0) complexes involving primary and secondary phosphines

Tom Campbell, Alexander M. Gibson, Richard Hart, Simon D. Orchard, Simon J.A. Pope, Gillian Reid *

Department of Chemistry, University of Southampton, Highfield, Southampton SO17 1BJ, UK

Received 2 August 1999; accepted 17 September 1999

Abstract

$[M(CO)_6]$ (M = Mo or W) reacts with 4.5 molar equivalents of L ($L = PPh_2H$ or $PPhH_2$) in excess ethanolic $NaBH_4$ to yield the *fac*-trisubstituted species $[M(CO)_3(L)_3]$ in good yield, with no evidence for species with lower degrees of substitution. IR, ^1H-, $^{13}C\{^1H\}$-, $^{31}P\{^1H\}$- and ^{95}Mo-NMR spectroscopy on these compounds, together with X-ray crystallographic studies on two examples, confirm the *fac*-tricarbonyl arrangement both in solution and in the solid state. Similar reactions involving PCy_2H yield only the *cis*-disubstituted species $[M(CO)_4(PCy_2H)_2]$. Reaction of $[M'(CO)_4(nbd)]$ (M′ = Cr or Mo) or $[W(CO)_4(TMPA)$ (TMPA = tetramethylpropylenediamine) with two molar equivalents of L ($L = PPh_2H$, $PPhH_2$ or PCy_2H) or with one molar equivalent of L–L (L–L = *o*-$C_6H_4(PH_2)_2$, $PhHPCH_2CH_2PHPh$ or $PhHPCH_2CH_2CH_2PHPh$) in warm toluene solution give $[M'(CO)_4(L)_2]$, $[W(CO)_4(L)_2]$, $[M'(CO)_4(L–L)]$ or $[W(CO)_4(L–L)]$, respectively. Spectroscopic studies indicate that these all exist as *cis*-disubstituted species in solution and single-crystal X-ray analyses on three examples confirm this assignment in the solid state. The primary and secondary phosphines act as neutral two-electron donors in all cases with retention of the P–H functions. Trends in the spectroscopic and structural data are discussed.

Keywords: Chromium; Molybdenum; Tungsten; Primary phosphines; Secondary phosphines

1. Introduction

In contrast to the very extensive investigations of the coordination chemistry of mono-, bi- and polydentate tertiary phosphines, primary and secondary phosphine chemistry has received much less detailed study. Probably the main reason for this is that upon coordination of the P donor atom to a metal centre, the P–H bond is weakened significantly, and is thus susceptible to deprotonation giving phosphido species. Indeed this does occur in the reaction of MCl_2 (M = Pd or Pt) with PPh_2H, which yields the phosphido-bridged dimer $[M_2Cl_2(PPh_2H)_2(\mu\text{-}PPh_2)_2]$ [1]. Similarly, Au(I) salts react with PPh_2H or $PPhH_2$ to yield phosphido bridged polymers such as $[\{Au(\mu\text{-}PPh_2)\}_2]$ [2]. However, if the deprotonation can be controlled then complexes of primary and secondary phosphines can act as suitable templates for the synthesis of multidentate and macrocyclic phosphines. Thus, for example Stelzer and co-workers have used this approach in the preparation of tetraphosphine macrocycles, e.g. via the Pd(II) template species $[Pd(MeHPCH_2CH_2PHMe)_2]^{2+}$ [3], while Norman and co-workers and Edwards and co-workers used a radical initiated cyclisation procedure on the Mo(0) template species *fac*-$[Mo(CO)_3(H_2PCH_2CH{=}CH_2)_3]$ to generate the macrocyclic triphosphine [12]aneP_3 (1,5,9-triphosphacyclododecane) and derivatives in high yield [4]. Despite the crucial role played by the primary or secondary phosphine complexes in these important reactions, there is still relatively little known about the coordination chemistry of PR_2H or PRH_2 to metal centres. We have investigated the coordination chemistry of these ligands with a variety of middle and late transition metal ions, including Mn(I), Rh(III), Ru(II), Os(II), Ni(II), Pd(II) and Pt(II) [5–9]. Through this

* Corresponding author. Fax: +44-1703-593-781.
E-mail address: gr@soton.ac.uk (G. Reid)

0022-328X/99/$ - see front matter
PII: S0022-328X(99)00570-7

work we have generated a range of species in which the PR_2H or PRH_2 ligands behave as neutral two-electron donors. We report here the synthesis and spectroscopic (including ^{1}H-, ^{13}C{^{1}H}-, ^{31}P{^{1}H}- and ^{95}Mo-NMR) characterisation of a series of di- and tri-substituted complexes *fac*-[M(CO)$_3$L$_3$] (M = Mo or W; L = PPh_2H or $PPhH_2$), *cis*-[M(CO)$_4$L$_2$] (M = Cr, Mo or W; L = PPh_2H, PCy_2H or $PPhH_2$) and *cis*-[Mo(CO)$_4$(L–L)] (L–L = $PhHPCH_2CH_2PHPh$, $PhHPCH_2CH_2CH_2PHPh$ or *o*-$C_6H_4(PH_2)_2$). Reaction of [M(CO)$_6$] with excess phosphine in ethanolic $NaBH_4$ produces the *fac* or the *cis* species, depending upon the nature of the phosphine, while the *cis* species form by substitution of nbd or TMPA from the appropriate tetracarbonyl precursor species. Single-crystal X-ray structure determinations on *fac*-[Mo(CO)$_3$($PPhH_2$)$_3$], *fac*-[W(CO)$_3$(PPh_2H)$_3$], *cis*-[Cr(CO)$_4$(PPh_2H)$_2$], *cis*-[Mo(CO)$_4$($PPhH_2$)$_2$] and *cis*-[W(CO)$_4$(PPh_2H)$_2$] are also described and trends in the data are discussed. The preparations of [Cr(CO)$_4$($PPhH_2$)$_2$], [Mo(CO)$_4$($PPhH_2$)$_2$], [Mo(CO)$_4$(PPh_2H)$_2$] and [Mo(CO)$_3$(PPh_2H)$_3$] have been reported previously, however, since this was in the 1960s and early 1970s, their spectroscopic and structural characterisation were rather limited [10], although the crystal structure of *fac*-[Mo(CO)$_3$(PPh_2H)$_3$]·0.25hexane has been reported [11]. The preparation and spectroscopic characterisation of the complexes *cis*-[Mo(CO)$_4$($PhHPCH_2CH_2PHPh$)] and *cis*-[Mo(CO)$_4$($PhHPCH_2CH_2CH_2PHPh$)] have also been described [12]. We have resynthesised these disecondary phosphine complexes to obtain ^{95}Mo-NMR data and to allow comparisons with the other species.

2. Results and discussion

Reaction of [M(CO)$_6$] with 4.5 molar equivalents of L (L = PPh_2H or $PPhH_2$) in degassed EtOH solution in the presence of an excess of $NaBH_4$, gives the complexes *fac*-[M(CO)$_3$L$_3$] in moderate yield as pale yellow/fawn coloured solids. The reactions were followed by solution IR spectroscopy, and were considered to be complete when the CO bands associated with the hexacarbonyl metal precursor had completely disappeared. The fast-atom bombardment mass spectra (FAB MS) of the isolated products show highest mass peaks with the correct isotopic distributions corresponding to [M(CO)$_3$L$_3$]$^+$. Other peaks arising from fragmentation products generated via sequential loss of CO or L are also observed. As expected for *fac*-trisubstituted species, the IR spectra show two strong CO stretching vibrations (theory $a_1 + e$), as well as peaks due to coordinated ligand. Evidence for retention of the P-bound protons comes from the appearance of a weak peak at ca. 2300 cm^{-1} (ν_{PH}), and ^{1}H-NMR spectroscopy which reveals a very broad multiplet around 5–6 ppm due to P–H functions. Together with microanalytical data, these results indicate the formulation *fac*-[M(CO)$_3$L$_3$] for the products. Chatt and co-workers have used borohydride to activate the CO ligands in the preparation of a number of tertiary phosphine complexes of Mo– and W–tetracarbonyls [13], however, with PPh_2H and $PPhH_2$ we did not observe any compounds with lower degrees of carbonyl substitution under these reaction conditions. Similar reaction with PCy_2H does not yield *fac*-[M(CO)$_3$(PCy_2H)$_3$], but instead gives only *cis*-[M(CO)$_4$(PCy_2H)$_2$]. It is unlikely that this is due to steric constraints alone since we have recently [5] prepared *fac*-[Mn(CO)$_3$(PCy_2H)$_3$]$^+$, which incorporates three mutually *fac*-PCy_2H ligands. The compound *fac*-[Mo(CO)$_3$(PPh_2H)$_3$] has been previously synthesised by the reaction of [Mo(CO)$_3$(C_7H_8)] (C_7H_8 = cycloheptatriene) and PPh_2H in refluxing toluene and our spectroscopic data are consistent with those reported [10].

The *cis*-disubstituted species [M(CO)$_4$L$_2$] (M = Cr, Mo, W; L = PPh_2H, PCy_2H, $PPhH_2$) are formed by treatment of *cis*-[M(CO)$_4$(nbd)] (M = Cr, Mo; nbd = norbornadiene) or *cis*-[W(CO)$_4$(TMPA)] (TMPA = $Me_2N(CH_2)_3NMe_2$) with two molar equivalents of L in CH_2Cl_2 solution. While *cis*-[M(CO)$_4$(piperidine)$_2$] (M = Mo or W) react similarly to yield the desired species, typically we found that poorer yields were obtained from this route. *cis*-[Mo(CO)$_4$(L–L)] (L–L = $PhHPCH_2CH_2PHPh$, $PhHPCH_2CH_2CH_2PHPh$ or *o*-$C_6H_4(PH_2)_2$) were prepared similarly from [Mo(CO)$_4$(nbd)] and L–L. [Mo(CO)$_4$($PhHPCH_2CH_2PHPh$)] and [Mo(CO)$_4$($PhHPCH_2CH_2CH_2PHPh$)] were prepared previously via the reaction of [Mo(CO)$_6$] and the phosphine in refluxing diglyme [12].

Mass spectra were obtained either by FAB or APCI, and show peaks with the correct isotopic distribution for [M(CO)$_4$L$_2$] (or [Mo(CO)$_4$(L–L)]) as well as fragment ions consistent with loss of CO or L (or L–L). Solution IR spectroscopy shows (Table 1) four ν(CO) stretching vibrations consistent with the *cis*-disubstituted species (theory $2a_1 + b_1 + b_2$) and our data are consistent with the literature data for those compounds previously reported [10]. There is also evidence for coordinated L and P–H functions from IR spectroscopy (KBr disk). The ^{1}H-NMR spectra confirm the presence of the primary or secondary phosphines and show a broad multiplet around 5–6 ppm due to the P–H protons.

^{31}P{^{1}H}-, ^{95}Mo- and ^{13}C{^{1}H}-NMR spectroscopic data were recorded for the compounds. The ^{13}C{^{1}H}-NMR spectra show resonances associated with the Ph or Cy groups on the phosphine ligands. In addition we observe ^{31}P coupling to the CO resonances. For the *fac*-species δ(CO) appears as a doublet of triplets due to coupling to the magnetically non-equivalent phos-

phines, while for the *cis* compounds two CO environments are observed, a triplet corresponding to the CO ligands *cis* to the phosphines and a doublet of doublets due to the CO ligands *trans* to phosphine. δ(CO) for the former lies to a lower frequency. The *cis* $^{13}C-^{31}P$ couplings (ca. 8–15 Hz) are consistently smaller than the *trans* couplings (ca. 20–30 Hz).

The $^{31}P\{^{1}H\}$-NMR spectra each show a singlet resonance (except the disecondary phosphine complexes — see below) indicative of equivalent P environments and these occur to high frequency of the uncoordinated phosphine. There is a shift of $\delta(^{31}P)$ to high frequency with an increasing degree of substitution at the metal centre, and a shift to low frequency from Cr → Mo → W. For the molybdenum species coupling to $^{95/97}Mo$ (^{95}Mo: $I = 5/2$. 15.7%, $Q = 0.12 \times 10^{-28}$ m^2; ^{97}Mo: $I = 5/2$, 9.5%, $Q = 1.1 \times 10^{-28}$ m^2) is clearly evident for the *fac*-species, giving a six-line satellite pattern, suggesting that the electric field gradient at Mo in these C_{3v} species is very small. In contrast, no $^{95/97}Mo$ coupling is observed in the $^{31}P\{^{1}H\}$-NMR spectra of the *cis*-disubstituted Mo species (C_{2v}). For the diphosphine species we observe the expected trend in $\delta(^{31}P)$ with chelate ring size [14].

Two stereoisomers are possible for the disecondary phosphine complexes (*meso* and DL), and hence we observe these by NMR spectroscopy. For [Mo(CO)$_4$(PhHPCH$_2$CH$_2$PHPh)] we observe both stereoisomers in ca. 1:1 ratio, $\delta(^{31}P)$ 18.5, 21.0, while for [Mo(CO)$_4$(PhHPCH$_2$CH$_2$CH$_2$PHPh)] one of the stereoisomers (*meso*) dominates ($\delta(^{31}P)$ −6.9, >95%), consistent with the ratio of the *meso*:DL forms in the free diphosphine. The ^{31}P-NMR data for these disecondary phosphine complexes compare well with the literature data [12]. For the tungsten complexes we observed ^{183}W satellites on all of the resonances (^{183}W: $I = 1/2$, 14.4%).

For all of the Group 6 species studied the ^{1}H-coupled ^{31}P-NMR spectra reveal either broad doublets or broad triplets due to coupling between the ^{31}P and the directly bound ^{1}H nuclei, $^{1}J_{PH}$ ca. 320 Hz (there is also evidence for coupling to the Ph and Cy ring protons).

^{95}Mo-NMR spectra for the *fac*-species each show a quartet consistent with coupling to three equivalent P nuclei, while the *cis*-species show a triplet. $\delta(^{95}Mo)$ for the substituted complexes typically lies to a higher frequency than that for [Mo(CO)$_6$] (−1856 [15]), with the trisubstituted species at higher frequencies than the disubstituted derivatives, consistent with the trends in the literature [16]. The resonance for the disecondary and diprimary phosphine complexes which involve five-membered chelate rings, lie to low frequency compared with the other Mo species studied, (including the PhHPCH$_2$CH$_2$CH$_2$PHPh complex which involves a six-membered chelate ring), and rather closer to [Mo(CO)$_6$] itself. However, the ^{31}P coupling establishes unequivocally the assignments for these resonances. For [Mo(CO)$_4$(PhHPCH$_2$CH$_2$PHPh)] two triplets are observed due to the *meso* and DL stereoisomers, $\delta(^{95}Mo) = -1847$, $^{1}J_{MoP} = 128$ Hz and $\delta(^{95}Mo) = -1860$, $^{1}J_{MoP} = 123$ Hz, while for [Mo(CO)$_4$(PhHPCH$_2$CH$_2$CH$_2$PHPh)] we observe one triplet at −1779 ppm ($^{1}J_{MoP} = 125$ Hz), assigned to the *meso* isomer. The coupling constants are comparable with those reported for other Mo(0) phosphines [16].

In order to confirm the stereochemistries at the metal centres and to establish structural trends, single-crystal X-ray structure analyses were undertaken on *fac*-[Mo(CO)$_3$(PPhH$_2$)$_3$], *fac*-[W(CO)$_3$(PPh$_2$H)$_3$], *cis*-[Cr(CO)$_4$(PPh$_2$H)$_2$], *cis*-[Mo(CO)$_4$(PPhH$_2$)$_2$] and *cis*-[W(CO)$_4$(PPh$_2$H)$_2$]. The crystal structure of [Mo(CO)$_3$-

Table 1
$^{31}P\{^{1}H\}$- and ^{95}Mo-NMR and IR spectroscopic data [a]

Compound	δ ^{31}P (ppm)	δ ^{95}Mo (ppm)	J_{MP} (Hz) [b]	ν_{CO} (cm^{-1})
cis-[Cr(CO)$_4$(PPh$_2$H)$_2$]	+42.3			2014, 1919sh, 1901, 1886sh
cis-[Cr(CO)$_4$(PPhH$_2$)$_2$]	−27.5			2019, 1923sh, 1907, 1893sh
cis-[Cr(CO)$_4$(PCy$_2$H)$_2$]	+53.4			2001, 1901sh, 1883, 1866sh
fac-[Mo(CO)$_3$(PPh$_2$H)$_3$]	+22.0	−1639*q*	105	1947, 1855
fac-[Mo(CO)$_3$(PPhH$_2$)$_3$]	−53.5	−1702*q*	121	1957, 1866
cis-[Mo(CO)$_4$(PPh$_2$H)$_2$]	+14.5	−1724*t*	130	2026, 1926*sh*, 1914, 1892*sh*
cis-[Mo(CO)$_4$(PPhH$_2$)$_2$]	−60.5	−1769*t*	124	2030, 1930*sh*, 1918, 1897*sh*
cis-[Mo(CO)$_4$(PCy$_2$H)$_2$]	+25.0	−1810*t*	132	2014, 1909*sh*, 1894, 1872*sh*
cis-[Mo(CO)$_4$(PhHPCH$_2$CH$_2$PHPh)]	18.5, 21.0	−1847*t*, −1860*t*	128, 123	2024, 1926*sh*, 1908, 1891*sh*
cis-[Mo(CO)$_4$(PhHPCH$_2$CH$_2$CH$_2$PHPh)]	−6.9	−1779*t*	125	2023, 1924*sh*, 1903, 1888*sh*
cis-[Mo(CO)$_4${*o*-C$_6$H$_4$(PH$_2$)$_2$}]	−44.1	−1891*t*	120	2032, 1935*sh*, 1919, 1903*sh*
fac-[W(CO)$_3$(PPh$_2$H)$_3$]	+4.3		217	1942, 1851
fac-[W(CO)$_3$(PPhH$_2$)$_3$]	−72.0		209	1951, 1858
cis-[W(CO)$_4$(PPh$_2$H)$_2$]	−4.6		227	2022, 1917*sh*, 1903, 1885*sh*
cis-[W(CO)$_4$(PPhH$_2$)$_2$]	−80.9		200	2026, 1907*sh*, 1875, 1864*sh*
cis-[W(CO)$_4$(PCy$_2$H)$_2$]	+8.6		214	2010, 1904*sh*, 1883, 1860*sh*

[a] Spectra were recorded at 300 K in $CDCl_3$ solution.
[b] Refers to $^{1}J(^{95}Mo-^{31}P)$ or $^{1}J(^{185}W-^{31}P)$ as appropriate.

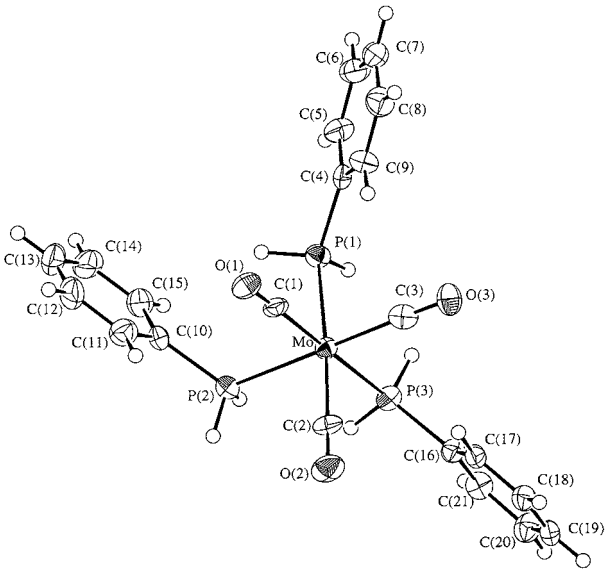

Fig. 1. View of the structure of *fac*-$[Mo(CO)_3(PPhH_2)_3]$ with numbering scheme adopted. Ellipsoids are drawn at 40% probability.

Table 2
Selected bond lengths (Å) and bond angles (°) for *fac*-$[Mo(CO)_3(PPhH_2)_3]$

Bond lengths			
Mo–P(1)	2.501(3)	Mo–P(2)	2.493(3)
Mo–P(3)	2.500(3)	Mo–C(1)	1.99(l)
Mo–C(2)	1.972(10)	Mo–C(3)	1.97(1)
Bond angles			
P(1)–Mo–P(2)	87.35(9)	P(1)–Mo–P(3)	86.78(9)
P(1)–Mo–C(1)	92.2(3)	P(1)–Mo–C(2)	174.8(3)
P(1)–Mo–C(3)	92.9(3)	P(2)–Mo–P(3)	90.08(10)
P(2)–Mo–C(1)	89.5(3)	P(2)–Mo–C(2)	87.8(3)
P(2)–Mo–C(3)	179.2(3))	P(3)–Mo–C(1)	178.9(2)
P(3)–Mo–C(2)	91.4(3)	P(3)–Mo–C(3)	90.7(3)
C(1)–Mo–C(2)	89.5(4)	C(1)–Mo–C(3)	89.8(4)
C(2)–Mo–C(3)	92.1(4)		

$(PPhH_2)_3]$ shows a discrete neutral molecule in the asymmetric unit, (Fig. 1, Table 2) with the primary phosphine ligands in a *fac* arrangement giving a distorted octahedral geometry at Mo, Mo–P = 2.493(3)–2.501(3), Mo–C = 1.97(1)–1.99(1) Å. The *cis* angles around the metal centre lie in the range 86.78(9)–92.9(3)°. The crystal structure of $[W(CO)_3(PPh_2H)_3]$ also confirms the *fac* arrangement of the phosphine ligands (Fig. 2, Table 3) giving a very similar overall geometry, with W–P = 2.490(4)–2.504(3), W–C = 1.95(1)–1.97(1) Å. The M–P and M–C bond lengths in these species are not significantly different, reflecting the similarity of the Mo(0) and W(0) radii.

The crystal structures of the disubstituted species $[Cr(CO)_4(PPh_2H)_2]$ (Fig. 3, Table 4), $[Mo(CO)_4(PPhH_2)_2]$ (Fig. 4, Table 5) and $[W(CO)_4(PPh_2H)_2]$ (Fig. 5, Table 6) each confirm a *cis*-disubstituted arrangement at the metal centre, giving a distorted octahedral geometry and confirming the structure deduced spectroscopically in solution. The $M–C_{trans\ CO}$ bond distances in these compounds are longer than those *trans* to P, a trend observed previously for *cis*-$[M(CO)_4(PR_3)_2]$ [17].

Importantly, in a number of these structures (see Section 3) the integrity of the P–H functions was confirmed crystallographically with the H atoms being located from the difference map, thus these primary and secondary phosphines behave as neutral two-electron donors to Group 6 metal carbonyls.

Comparing the data for $[Mo(CO)_3(PPhH_2)_3]$ with that for $[Mo(CO)_4(PPhH_2)_2]$ shows that the Mo–P bond lengths are virtually insensitive to the degree of substitution at Mo. This is also true for the tungsten–diphenylphosphine derivatives. The Mo–P distances and the bond angles around Mo in the previously characterised *fac*-$[Mo(CO)_3(PPh_2H)_3].0.25C_6H_{14}$ (Mo–

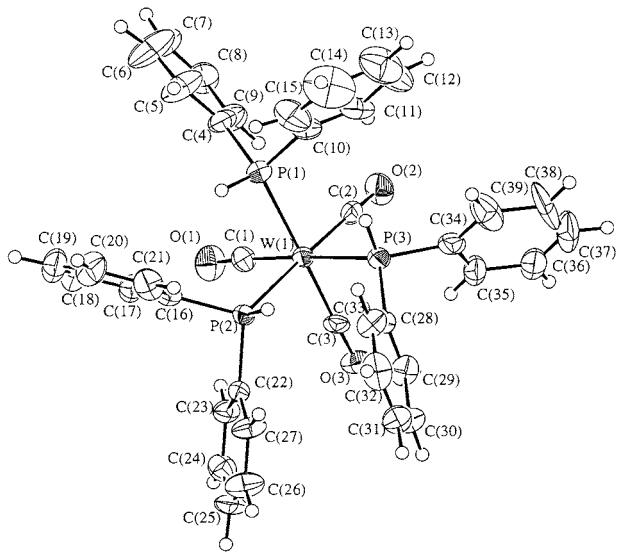

Fig. 2. View of the structure of *fac*-$[W(CO)_3(PPh_2H)_3]$ with numbering scheme adopted. Ellipsoids are drawn at 40% probability.

Table 3
Selected bond lengths (Å) and bond angles (°) for *fac*-$[W(CO)_3(PPh_2H)_3]$

Bond lengths			
W(1)–P(1)	2.490(4)	W(1)–P(2)	2.504(3)
W(1)–P(3)	2.493(3)	W(1)–C(1)	1.95(1)
W(1)–C(2)	1.97(1)	W(1)–C(3)	1.97(1)
Bond angles			
P(1)–W(1)–P(2)	87.5(1)	P(1)–W(1)–P(3)	90.9(1)
P(1)–W(1)–C(1)	91.2(4)	P(1)–W(1)–C(2)	93.5(4)
P(1)–W(1)–C(3)	178.6(4)	P(2)–W(1)–P(3)	86.6(1)
P(2)–W(1)–C(1)	92.4(4)	P(2)–W(1)–C(2)	177.9(3)
P(2)–W(1)–C(3)	93.0(4)	P(3)–W(1)–C(1)	177.7(4)
P(3)–W(1)–C(2)	91.6(4)	P(3)–W(1)–C(3)	90.5(4)
C(1)–W(1)–C(2)	89.4(5)	C(1)–W(1)–C(3)	87.4(5)
C(2)–W(1)–C(3)	86.1(5)		

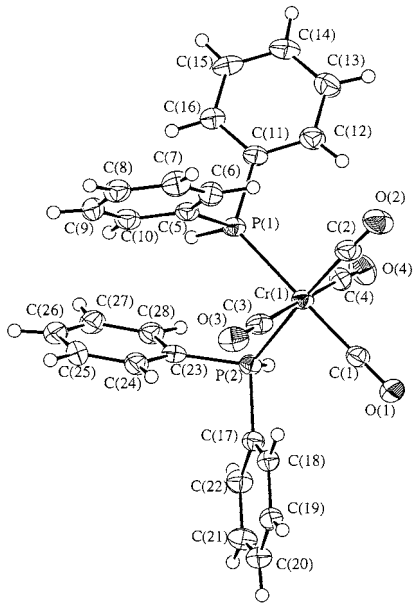

Fig. 3. View of the structure of *cis*-$[Cr(CO)_4(PPh_2H)_2]$ with numbering scheme adopted. Ellipsoids are drawn at 40% probability.

Table 4
Selected bond lengths (Å) and bond angles (°) for *cis*-$[Cr(CO)_4(PPh_2H)_3]$

Bond lengths			
Cr(1)–P(1)	2.359(2)	Cr(1)–P(2)	2.347(2)
Cr(1)–C(1)	1.867(4)	Cr(1)–C(2)	1.857(5)
Cr(1)–C(3)	1.897(4)	Cr(1)–C(4)	1.891(4)
Bond angles			
P(1)–Cr(1)–P(2)	91.98(9)	P(1)–Cr(1)–C(1)	177.9(1)
P(1)–Cr(1)–C(2)	91.1(2)	P(1)–Cr(1)–C(3)	87.9(1)
P(1)–Cr(1)–C(4)	90.9(1)	P(2)–Cr(1)–C(1)	89.5(1)
P(2)–Cr(1)–C(2)	176.7(1)	P(2)–Cr(1)–C(3)	89.2(1)
P(2)–Cr(1)–C(4)	85.2(1)	C(1)–Cr(1)–C(2)	87.4(2)
C(1)–Cr(1)–C(3)	90.7(2)	C(1)–Cr(1)–C(4)	90.6(2)
C(2)–Cr(1)–C(3)	92.1(2)	C(2)–Cr(1)–C(4)	93.6(2)
C(3)–Cr(1)–C(4)	174.2(2)		

P = 2.490(3)–2.506(4), Mo–C = 1.930(12)–1.940(13) Å, < P–Mo–P = 85.2(1)–87.9(1)°) [11] compare closely with the bond length and angle distributions for *fac*-$[Mo(CO)_3(PPhH_2)_3]$ reported here, indicating that the differing cone angles of the phosphines in these species have little effect upon the geometry at Mo.

3. Experimental

Infrared spectra were measured in CH_2Cl_2 solution using a Perkin–Elmer 1600 FTIR over the range 2200–1700 cm^{-1} or as KBr or CsI discs using a Perkin–Elmer 983 spectrometer over the range 4000–200 cm^{-1}. Mass spectra were run by electron impact or FAB using 3-NOBA (3-nitrobenzyl alcohol) as matrix on a VG Analytical 70-250-SE Normal Geometry Double Focusing Mass Spectrometer or by APCI using a VG Biotech platform. ^{1}H-NMR spectra were recorded in $CDCl_3$ using a Bruker AM300 spectrometer. $^{31}P\{^1H\}$-, $^{95}Mo\{^1H\}$- and $^{13}C\{^1H\}$-NMR spectra were recorded in CH_2Cl_2 containing ca. 10–15% $CDCl_3$ using a Bruker AM360 spectrometer operating at 145.8, 23.48 or 90.55 MHz, respectively, and are referenced to 85% H_3PO_4, aqueous $Na_2[MoO_4]$ and Me_4Si, respectively ($\delta = 0$). [Cr(acac)$_3$] was added to the NMR solu-

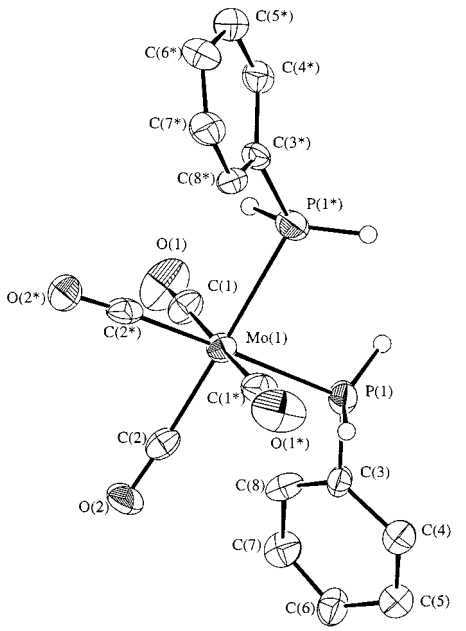

Fig. 4. View of the structure of *cis*-$[Mo(CO)_4(PPhH_2)_2]$ with numbering scheme adopted. Ellipsoids are drawn at 40% probability. Only one of the two equally probable orientations for the disordered phenyl rings is shown.

Table 5
Selected bond lengths (Å) and bond angles (°) for *fac*-$[Mo(CO)_4(PPhH_2)_2]$

Bond lengths			
Mo(1)–P(1)	2.508(3)	Mo(1)–P(1)	2.508(3)
Mo(1)–C(1)	2.06(1)	Mo(1)–C(1)	2.06(1)
Mo(1)–C(2)	1.98(1)	Mo(1)–C(2)	1.98(1)
Bond angles			
P(1)–Mo(1)–P(1)	87.9(1)	P(1)–Mo(1)–C(1)	89.8(3)
P(1)–Mo(1)–C(1)	89.5(3)	P(1)–Mo(1)–C(2)	93.5(3)
P(1)–Mo(1)–C(2)	178.6(3)	P(1)–Mo(1)–C(1)	89.5(3)
P(1)–Mo(1)–C(1)	89.8(3)	P(1)–Mo(1)–C(2)	178.6(3)
P(1)–Mo(1)–C(2)	93.5(3)	C(1)–Mo(1)–C(1)	179.0(6)
C(1)–Mo(1)–C(2)	90.2(5)	C(1)–Mo(1)–C(2)	90.6(4)
C(1)–Mo(1)–C(2)	90.6(4)	C(1)–Mo(1)–C(2)	90.2(5)
C(2)–Mo(1)–C(2)	85.2(6)		

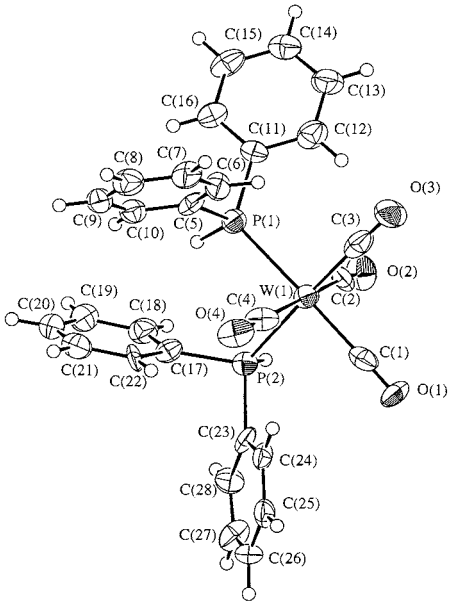

Fig. 5. View of the structure of *cis*-$[W(CO)_4(PPh_2H)_2]$ with numbering scheme adopted. Ellipsoids are drawn at 40% probability.

Table 6
Selected bond lengths (Å) and bond angles (°) for *fac*-$[W(CO)_4(PPh_2H)_2]$

Bond lengths			
W(1)–P(1)	2.467(4)	W(1)–P(2)	2.513(4)
W(1)–C(1)	2.01(2)	W(1)–C(2)	2.02(2)
W(1)–C(3)	2.03(2)	W(1)–C(4)	2.03(2)
Bond angles			
P(1)–W(1)–P(2)	89.6(1)	P(1)–W(1)–C(1)	177.3(5)
P(1)–W(1)–C(2)	91.0(5)	P(1)–W(1)–C(3)	92.5(4)
P(1)–W(1)–C(4)	87.0(5)	P(2)–W(1)–C(1)	90.7(5)
P(2)–W(1)–C(2)	83.4(5)	P(2)–W(1)–C(3)	177.5(5)
P(2)–W(1)–C(4)	89.9(5)	C(1)–W(1)–C(2)	91.7(6)
C(1)–W(1)–C(3)	87.3(6)	C(1)–W(1)–C(4)	90.3(7)
C(2)–W(1)–C(3)	95.2(6)	C(2)–W(1)–C(4)	173.0(7)
C(3)–W(1)–C(4)	91.6(7)		

tions prior to recording $^{13}C\{^1H\}$-NMR spectra and a pulse delay of 2 s was introduced to accommodate the long relaxation times. Microanalyses were performed by the University of Strathclyde microanalytical service. $[Mo(CO)_4(nbd)]$, $[Cr(CO)_4(nbd)$ and $[W(CO)_4(TMPA]$ were prepared according to literature procedures [18,19].

3.1. Preparations

3.1.1. *fac*-$[Mo(CO)_3(PPh_2H)_3]$

To a degassed solution of $[Mo(CO)_6]$ (0.75 g, 2.61 mmol) and $NaBH_4$ (0.45 g, 11.7 mmol) in EtOH (70 cm^3), PPh_2H (1.5 g, 7.8 mmol) in EtOH (20 cm^3) were added dropwise over ca. 20 min. The resulting mixture was refluxed for 19 h. After cooling, the reaction volume was reduced to ca. 20 cm^3 in vacuo to give a pale yellow precipitate. This solid was filtered and washed with heptane and dried in vacuo. The compounds was recrystallised from CH_2Cl_2–diethyl ether. Yield 1.79 g, 91%. Required for $[C_{39}H_{33}MoO_3P_3]$: C, 63.4, H, 4.5. Found: C, 63.9; H, 4.8%. FAB MS (3-NOBA matrix): Found $m/z = 526$, 470, 313, 284; Calc. for $[^{98}Mo(CO)_2(PPh_2H)_2]^+$ $m/z = 526$, $[^{98}Mo(PPh_2H)_2]^+$ $m/z = 469$, $[^{98}Mo(CO)(PPh_2H)_2]^+$ $m/z = 313$; $[^{98}Mo(PPh_2H)]^+$ $m/z = 283$. ^{1}H-NMR: δ 7.43–7.17 (*m*, Ph, 10H), 5.55 (*m*, P*H*, 1H). $^{13}C\{^1H\}$-NMR: δ 219.0 (*dt*, *C*O), 128–135 (Ph).

3.1.2. *fac*-$[Mo(CO)_3(PPhH_2)_3]$

Pale yellow solid. Yield 65%. Required for $[C_{21}H_{21}MoO_3P_3]$: C, 49.4; H, 4.2. Found: C, 50.0, H, 4.6%. ^{1}H-NMR: δ 7.4–7.1 (*m*, Ph, 5H), 5.3 (*m*, P*H*, 2H). $^{13}C\{^1H\}$-NMR: δ 217.9 (*dt*, *C*O), 128–133 (Ph).

3.1.3. *fac*-$[W(CO)_3(PPh_2H)_3]$

Fawn solid. Yield 23%. Required for $[C_{39}H_{33}WO_3P_3]\cdot CHCl_3$: C, 50.8; H, 3.6. Found: C, 50.7; H, 5.2%. FAB MS (3-NOBA matrix): Found $m/z = 826$, 797, 769, 610, 554, 454, 398, 368; Calc. for $[^{183}W(CO)_3(PPh_2H)_3]^+$ $m/z = 825$, $[^{183}W(CO)_2(PPh_2H)_3]^+$ $m/z = 797$, $[^{183}W(CO)(PPh_2H)_3]^+$ $m/z = 769$; $[^{183}W(CO)_2(PPh_2H)_2]^+$ $m/z = 609$; $[^{183}W(PPh_2H)_2]^+$ $m/z = 553$; $[^{183}W(CO)_3(PPh_2H)]^+$ $m/z = 453$; $[^{183}W(CO)(PPh_2H)]^+$ $m/z = 397$; $[^{183}W(PPh_2H)]^+$ $m/z = 367$. ^{1}H-NMR: δ 7.5–7.2 (*m*, Ph, 10H), 5.8 (*m*, P*H*, 1H). $^{13}C\{^1H\}$-NMR: δ 211.3 (*dt*, *C*O), 128–135 (Ph).

3.1.4. *fac*-$[W(CO)_3(PPhH_2)_3]$

Fawn solid. Yield 33%. Required for $[C_{21}H_{21}WO_3P_3]$: C, 42.1; H, 3.5%. Found: C, 42.1, H, 3.8%. Electrospray MS: Found $m/z = 598$; Calc. for $[^{183}W(CO)_3(PPhH_2)_3]^+$ $m/z = 597$. ^{1}H-NMR: δ 7.43–7.13 (*m*, Ph, 5H), 5.83 (*m*, P*H*, 2H). $^{13}C\{^1H\}$-NMR: δ 209.1 (*dt*, *C*O), 126–134 (Ph).

3.1.5. *cis*-$[Cr(CO)_4(PPh_2H)_2]$

$[Cr(CO)_4(nbd)]$ (0.15 g, 0.586 mmol) was dissolved in stirring, degassed toluene (50 ml). PPh_2H (0.218 g, 1.172 mmol) was dissolved in degassed toluene (10 ml) and added dropwise to the solution under a dinitrogen atmosphere. The reaction mixture was stirred and heated to approximately 40°C for 24 h, or until solution IR studies showed the absence of bands associated with the starting material. The solvent was removed in vacuo and the resulting residue redissolved in the minimum volume of CH_2Cl_2. Cold hexane was added (10 ml) and the solution stored at -15°C. The resulting pale yellow crystalline solid was filtered and dried in vacuo. Yield = 0.242 g, 77%. Required for $[C_{28}H_{22}CrO_4P_2.CH_2Cl_2]$: C, 56.0; H, 3.9. Found: C, 56.1; H, 3.8%. APCI MS (MeCN): Found $m/z = 548$, 507, 424; Calc. for $[^{52}Cr(CO)_4(PPh_2H)_2]\cdot MeCN^+$ $m/z = 548$,

$[^{52}Cr(CO)_3(PPh_2H)_2]^+$ $m/z = 507$, $[^{52}Cr(PPh_2H)_2]^+$ $m/z = 424$. ^{1}H-NMR: δ 7.2–7.6 (*m*, Ph, 10H), 6.1 (*m*, P*H*, 1H). $^{13}C\{^1H\}$-NMR: δ 226.5 (*dd*, CO), 220.0 (*t*, CO), 128.7–133.6 (Ph).

3.1.6. cis-[Cr(CO)$_4$(PCy$_2$H)$_2$]

Pale yellow solid. Yield = 68%. Required for $[C_{28}H_{46}CrO_4P_2]$: C, 60.0; H, 8.2. Found: C, 60.5; H, 8.7%. APCI MS (MeCN): Found $m/z = 561$, 279; Calc. for $[^{52}Cr(CO)_4(PCy_2H)_2]^+$ $m/z = 561$, $[^{52}Cr(CO)(PCy_2H)]^+$ $m/z = 279$. ^{1}H-NMR: δ 4.7 (*m*, P*H*, 1H), 1.2–2.2 (*m*, Cy, 22H). $^{13}C\{^1H\}$-NMR: δ 227.5 (*dd*, CO) 222.3 (*t*, CO), 13.6–35.7 (Cy).

3.1.7. cis-[Cr(CO)$_4$(PPhH$_2$)$_2$]

Pale yellow solid. Yield = 88%. Required for $[C_{16}H_{14}CrO_4P_2]$: C, 50.0; H, 3.6. Found: C, 49.8; H, 3.8%. APCI MS (MeCN): Found $m/z = 384$, 272; Calc. for $[^{52}Cr(CO)_4(PPh_2H)_2]^+$ $m/z = 384$, $[^{52}Cr(CO)_4(PPh_2H)]^+$ $m/z = 272$. ^{1}H-NMR: δ 7.4–7.6 (*m*, Ph, 5H), 5.3 (*m*, P*H*, 2H). $^{13}C\{^1H\}$-NMR: δ 225.3 (*dd*, CO), 219.4 (*t*, CO), 127.4–132.2 (Ph).

3.1.8. cis-[Mo(CO)$_4$(PPh$_2$H)$_2$]

$[Mo(CO)_4(nbd)]$ (0.100 g, 0.333 mmol) was dissolved in stirring, degassed toluene (50 ml). PPh_2H (0.124 g, 0.666 mmol) was dissolved in degassed toluene (10 ml) and added dropwise to the solution under a dinitrogen atmosphere. The reaction mixture was stirred in the absence of light for 24 h, or until solution IR studies showed the absence of bands associated with the starting material. The solvent was removed in vacuo and the resulting residue redissolved in the minimum volume of CH_2Cl_2. Cold hexane was added (10 ml) and the solution stored at −15°C. The resulting crystalline solid was filtered and dried in vacuo. Yield = 0.141 g, 73%. Pale yellow solid. Required for $[C_{28}H_{22}MoO_4P_2]$: C, 57.9; H, 3.8. Found: C, 57.5; H, 3.7%. FAB MS (3-NOBA matrix): Found $m/z = 582$, 554, 526, 470, 284; Calc. for $[^{98}Mo(CO)_4(PPh_2H)_2]^+$ $m/z = 582$, $[^{98}Mo(CO)_3(PPh_2H)_2]^+$ $m/z = 554$, $[^{98}Mo(CO)_2(PPh_2H)_2]^+$ $m/z = 526$, $[^{98}Mo(PPh_2H)_2]^+$ $m/z = 470$, $[^{98}Mo(PPh_2H)]^+$ $m/z = 284$. ^{1}H-NMR: δ 7.2–8.0 (*m*, Ph, 10H), 6.0 (*m*, P*H*, 1H). $^{13}C\{^1H\}$-NMR: δ 215.1 (*dd*, CO), 209.1 (*t*, CO), 126.8–135.9 (Ph).

3.1.9. cis-[Mo(CO)$_4$(PCy$_2$H)$_2$]

Pale yellow solid. Yield = 62%. Required for $[C_{28}H_{46}MoO_4P_2]$: C, 55.4; H, 7.6. Found: C, 55.2; H, 8.1%. FAB MS (3-NOBA matrix): Found $m/z = 606$, 578, 548, 518; Calc. for $[^{98}Mo(CO)_4(PCy_2H)_2]^+$ $m/z = 606$, $[^{98}Mo(CO)_3(PCy_2H)_2]^+$ $m/z = 578$, $[^{98}Mo(CO)_2(PCy_2H)_2]^+$ $m/z = 548$, $[^{98}Mo(CO)(PCy_2H)_2]^+$ $m/z = 518$. ^{1}H-NMR: δ 4.8 (*m*, P*H*, 1H), 1.1–2.3 (*m*, Cy, 22H). $^{13}C\{^1H\}$-NMR: δ 216.3 (*dd*, CO), 211.7 (*t*, CO), 24.5–35.8 (Cy).

3.1.10. cis-[Mo(CO)$_4$(PPhH$_2$)$_2$]

Pale yellow solid. Yield = 60%. Required for $[C_{16}H_{14}MoO_4P_2]$: C, 44.9; H, 3.3. Found: C, 44.8; H, 3.3%. APCI MS (MeCN): Found $m/z = 431$, 401, 373, 291; Calc. for $[^{98}Mo(CO)_4(PPhH_2)_2]^+$ $m/z = 430$, $[^{98}Mo(CO)_3(PPhH_2)_2]^+$ $m/z = 402$, $[^{98}Mo(CO)_2(PPhH_2)_2]^+$ $m/z = 374$, $[^{98}Mo(CO)_3(PPhH_2)]^+$ $m/z = 292$. ^{1}H-NMR: δ 7.3–7.6 (*m*, Ph, 5H), 5.3 (*m*, P*H*, 2H). $^{13}C\{^1H\}$-NMR: δ 213.4 (*dd*, CO), 208.0 (*t*, CO), 128.8–132.9 (Ph).

3.1.11. cis-[Mo(CO)$_4$(PhHP(CH$_2$)$_2$PHPh)]

Fawn solid. Yield = 86%. Required for $[C_{18}H_{16}MoO_4P_2]$: C, 44.9; H, 3.3. Found: C, 44.8; H, 3.3%. APCI MS (MeCN): Found $m/z = 399$; Calc. for $[^{98}Mo(CO)_2(PhHPCH_2CH_2PHPh)]^+$ $m/z = 400$. ^{1}H-NMR: δ 7.3–7.6 (*m*, Ph, 10H), 5.5 (*m*, P*H*, 2H), 2.5 (*m*, CH_2, 4H).

3.1.12. cis-[Mo(CO)$_4$(PhHP(CH$_2$)$_3$PHPh]

Fawn solid. Yield = 86%. Required for $[C_{19}H_{18}MoO_4P_2]$: C, 44.9; H, 3.3. Found: C, 44.8; H, 3.3%. APCI MS (MeCN): Found $m/z = 469$, 441, 413; Calc. for $[^{98}Mo(CO)_4(PhHPCH_2CH_2CH_2PHPh)]^+$ $m/z = 470$, $[^{98}Mo(CO)_3(PhHPCH_2CH_2CH_2PHPh)]^+$ $m/z = 442$, $[^{98}Mo(CO)_2(PhHPCH_2CH_2CH_2PHPh)]^+$ $m/z = 414$. ^{1}H-NMR: δ 7.3–7.7 (*m*, Ph, 10H), 5.6 (*m*, P*H*, 2H), 2.6 (br *m*, CH_2, 6H).

3.1.13. cis-[Mo(CO)$_4$(*o*-C$_6$H$_4$(PH$_2$)$_2$)]

Fawn solid. Yield = 86%. Required for $[C_{10}H_8MoO_4P_2].0.5\ CH_2Cl_2$: C, 32.1; H, 2.3. Found: C, 32.1; H, 2.0%. APCI MS (MeCN): Found $m/z = 348$, 323, 292; Calc. for $[^{98}Mo(CO)_4(o\text{-}C_6H_4(PH_2)_2)]^+$ $m/z = 352$, $[^{98}Mo(CO)_3(o\text{-}C_6H_4(PH_2)_2)]^+$ $m/z = 324$, $[^{98}Mo(CO)_2(o\text{-}C_6H_4(PH_2)_2)]^+$ $m/z = 296$. ^{1}H-NMR: δ 7.5–8.0 (*m*, *o*-C_6H_4, 4H), 5.6 (*m*, P*H*, 4H). $^{13}C\{^1H\}$-NMR: δ 215.1 (*dd*, CO), 207.4 (*t*, CO), 129.9–137.9 (Ph).

3.1.14. cis-[W(CO)$_4$(PPh$_2$H)$_2$]

$[W(CO)_4(TMPA)]$, (0.100 g, 0.233 mmol), was dissolved in stirring degassed toluene (50 ml). PPh_2H (0.087 g, 0.466 mmol) was dissolved in degassed toluene (10 ml) and added dropwise to the solution under a dinitrogen atmosphere. The reaction mixture was stirred and heated to approximately 60°C for 24 h, or until solution IR studies showed the absence of bands associated with the starting material. The solvent was removed in vacuo and the resulting residue redissolved in the minimum volume of CH_2Cl_2. Cold hexane was added (10 ml) and the solution stored at −15°C. The resulting fawn coloured crystalline solid was filtered and dried in vacuo. Yield = 0.100 g, 64%. Required for $[C_{28}H_{22}WO_4P_2]$: C, 50.4; H, 3.6. Found: C, 49.9; H, 3.3%. FAB MS (3-NOBA matrix): Found $m/z = 668$,

639, 612, 554, 454, 426, 398; Calc. for $[^{184}W(CO)_4(PPh_2H)_2]^+$ $m/z = 668$, $[^{184}W(CO)_3(PPh_2H)_2]^+$ $m/z = 639$, $[^{184}W(CO)_2(PPh_2H)_2]^+$ $m/z = 612$, $[^{184}W(PPh_2H)_2]^+$ $m/z = 554$, $[^{184}W(CO)_3(PPh_2H)]^+$ $m/z = 454$, $[^{184}W(CO)_2(PPh_2H)]^+$ $m/z = 426$, $[^{184}W(CO)(PPh_2H)]^+$ $m/z = 398$. ^{1}H-NMR: δ 7.0–7.5 (*m*, Ph, 10H), 6.3 (*m*, P*H*, 1H). $^{13}C\{^1H\}$-NMR: δ 205.6 (*dd*, CO), 201.0 (*t*, CO), 126.9–135.6 (Ph).

3.1.15. *cis*-[W(CO)$_4$(PCy$_2$H)$_2$]

Fawn solid. Yield = 54%. Required for $[C_{28}H_{46}WO_4P_2]$: C, 48.4; H, 6.6. Found: C, 47.4; H, 6.8%. FAB MS (3-NOBA matrix): Found $m/z = 692$, 664, 634, 604; Calc. for $[^{184}W(CO)_4(PCy_2H)_2]^+$ $m/z = 692$,. $[^{184}W(CO)_3(PPh_2H)_2]^+$ $m/z = 664$, $[^{184}W(CO)_2(PCy_2H)_2]^+$ $m/z = 636$, $[^{184}W(CO)(PCy_2)_2]^+$ $m/z = 606$. ^{1}H-NMR: δ 4.1 (*m*, P*H*, 1H), 1.2–2.2 (*m*, Cy, 22H). $^{13}C\{^1H\}$-NMR: δ 206.0 (*dd*, CO), 202.9 (*t*, CO), 23.8–36.4 (Cy).

3.1.16. *cis*-[W(CO)$_4$(PPhH$_2$)$_2$]

Fawn solid. Yield = 79%. Required for $[C_{16}H_{14}WO_4P_2]$: C, 37.2; H = , 2.71. Found: C, 37.5; H, 2.86%. APCI MS (MeCN): Found $m/z = 438$, 425, 397; Calc. for $[^{184}W(PPh)_2]\cdot MeCN^+$ $m/z = 441$, $[^{184}W(CO)(PPh)_2]^+$ $m/z = 428$, $[^{184}W(PPh)_2]^+$ $m/z = 400$. ^{1}H-NMR: δ 7.2–7.5 (*m*, Ph, 5H), 5.5 (*m*, P*H*, 2H). $^{13}C\{^1H\}$-NMR: δ 211.9 (*dd*, CO), 205.6 (*t*, CO), 125.2–130.1 (Ph).

3.2. X-ray crystallography

Details of the crystallographic data collection and refinement parameters are given in Table 7. The crystals were grown by vapour diffusion of diethyl ether onto solutions of the complexes in CH_2Cl_2 at ca. −15°C. Data collection used a Rigaku AFC7S four-circle diffractometer equipped with an Oxford Systems open-flow cryostat operating at 150 K, using graphite-monochromated Mo–K_α X-radiation (λ = 0.71073 Å). The data were corrected for absorption using psi-scans (except for $[Mo(CO)_3(PPhH_2)_3]$ — see below). The structures were solved by direct methods [20] ($[Mo(CO)_3(PPhH_2)_3]$) or heavy atom methods [21] (others) and developed by iterative cycles of full matrix least-squares and difference Fourier synthesis [22]. The weighting scheme $w^{-1} = \sigma^2(F)$ gave satisfactory agreement analyses.

Table 7
Crystallographic data

Complex	*fac*-[Mo(CO)$_3$(PPhH$_2$)$_3$]	*fac*-[W(CO)$_3$(PPh$_2$H)$_3$]	*cis*-[Cr(CO)$_4$(PPh$_2$H)$_2$]	*cis*-[Mo(CO)$_4$(PPhH$_2$)$_2$]	*cis*-[W(CO)$_4$(PPh$_2$H)$_2$]
Empirical formula	$C_{21}H_{21}MoO_3P_3$	$C_{39}H_{33}WO_3P_3$	$C_{28}H_{22}CrO_4P_2$	$C_{16}H_{14}MoO_4P_2$	$C_{28}H_{22}O_4P_2W$
Formula weight	510.26	826.46	536.42	428.17	668.8
Crystal size (mm)	0.75 × 0.15 × 0.15	0.70 × 0.60 × 0.10	0.71 × 0.50 × 0.40	0.57 × 0.55 × 0.20	0.85 × 0.21 × 0.12
Crystal system	Triclinic	Monoclinic	Monoclinic	Orthorhombic	Monoclinic
Space group	$P\bar{1}$	$P2_1/c$	$P2_1/c$	*Pbcn*	$P2_1/c$
Unit cell dimensions					
a (Å)	11.104(8)	11.652(3)	10.39(2)	11.06(2)	10.443(1)
b (Å)	16.26(1)	17.410(6)	17.438(9)	7.82(2)	17.286(3)
c (Å)	6.805(3)	18.108(4)	14.399(8)	20.75(2)	14.473(3)
α (°)	94.11(6)	90	90	90	90
β (°)	105.88(4)	91.76(2)	97.62(7)	90	95.16(1)
γ (°)	108.43(7)	90	90	90	90
V (Å^3)	1104(1)	3671(1)	2586(7)	1796(4)	2600.6(7)
Z	2	4	4	4	4
μ(Mo–K$_\alpha$) (cm^{-1})	8.29	33.15	5.98	9.21	46.88
Max./min. transmission	1.000, 0.409	1.000, 0.716	1.000, 0.806	1.000, 0.705	1.000, 0,536
Unique observed reflections	3903	6932	4687	1862	4704
R_{int} (based on F^2)	0.045	0.106	0.020		0.052
Observed reflections	2722	3749	3800	1332	3749
With [$I_o > n\sigma(I_o)$]	$n = 2.5$	$n = 3$	$n = 2$	$n = 2$	$n = 2$
Number of parameters	253	415	316	142	316
R [a]	0.072	0.048	0.051	0.081	0.075
R_w [b]	0.087	0.050	0.077	0.126	0.128
Max. residual peak (e Å^{-3})	1.35	1.12	0.52	0.72	1.74

[a] $R = \Sigma(|F_{obs}|_i - |F_{calc}|_i)/\Sigma|F_{obs}|_i$.

[b] $R_w = \sqrt{[\Sigma w_i(|F_{obs}|_i - |F_{calc}|_i)^2/\Sigma w_i|F_{obs}|_i^2]}$.

3.2.1. $[Mo(CO)_3(PPhH_2)_3]$

Psi-scans did not give a satisfactory absorption correction and therefore with the model at isotropic convergence the raw data were corrected for absorption using DIFABS [23]. All non-H atoms were refined anisotropically while H-atoms were placed in fixed, calculated positions. Selected bond lengths and angles are given in Table 1.

3.2.2. $[W(CO)_3(PPh_2H)_3]$

All non-H atoms were refined anisotropically while H-atoms were placed in fixed, calculated positions. Selected bond lengths and angles are given in Table 2.

3.2.3. $[Cr(CO)_4(PPh_2H)_2]$

An 8.8% decrease in the intensities of the standard reflections was observed, hence a linear decay correction was applied. All non-H atoms were refined anisotropically and H atoms were located from the difference map and included but not refined. Selected bond lengths and angles are given in Table 3.

3.2.4. $[Mo(CO)_4(PPhH_2)_2]$

The crystal quality was rather poor and this is reflected in the residuals. which are higher than normally expected. A 7.5% decrease in the intensity of the standard reflections occurred during data collection and a linear decay correction was therefore applied. The molecule possesses crystallographic *m* symmetry, with the Mo atom lying on the mirror plane (0, *y*, 1/4). Two alternative orientations (50:50 occupancy) were identified for the Ph rings, the disorder occurring via twisting about C(3) and C(6) both of which are fully occupied since they are shared by the two conformations. All non-H atoms were refined anisotropically, while the H atoms associated with the P atoms were located from the difference map and included, but not refined. The H atoms associated with the disordered Ph ring were omitted from the final structure factor calculation. Selected bond lengths and angles are given in Table 4.

3.2.5. $[W(CO)_4(PPh_2H)_2]$

A 5.5% decrease in the intensities of the standard reflections was observed, hence a linear decay correction was applied. All non-H atoms were refined anisotropically and H atoms were included in fixed, calculated positions. Selected bond lengths and angles are given in Table 5.

4. Supplementary material

Crystallographic data for the structural analysis has been deposited with the Cambridge Crystallographic Data Centre, CCDC reference numbers 132792–132796. Copies of this information may be obtained free of charge from the Director, CCDC, 12 Union Road, Cambridge, CB2 1EZ, UK (fax: +44-1223-336-033; e-mail: deposit@ccdc.cam.ac.uk or www: http://www.ccdc.cam.ac.uk).

Acknowledgements

The authors thank the EPSRC and the University of Southampton for support and Dr M. Webster for helpful discussions on the crystallography.

References

[1] (a) R.G. Hayter, J. Am. Chem. Soc. 84 (1962) 3046. (b) W. Levason, C.A. McAuliffe, Inorg. Chim. Acta 16 (1976) 167. (c) J.B. Brandon, K.R. Dixon, Can. J. Chem. 59 (1981) 1188. (d) A.J. Carty, F. Hartstock, N.J. Taylor, Inorg. Chem. 21 (1982) 1349. (e) T. Gebauer, G. Frenzen, K. Dehnicke, Z. Naturforsch. 47b (1992) 1505.
[2] (a) D.B. Dyson, R.V. Parish, C.A. McAuliffe, R.G. Pritchard, R. Fields, B. Beagley, J. Chem. Soc. Dalton Trans. (1989) 907. (b) A.M. Gibson, PhD Thesis, University of Southampton, 1997.
[3] D.J. Brauer, F. Gol, S. Hietkamp, H. Peters, W.S. Sheldrick, O. Stelzer, Chem. Ber. 119 (1986) 349.
[4] (a) B.N. Diel, R.C. Haltiwanger, A.D. Norman, J. Am. Chem. Soc. 104 (1982) 4700. (b) S.J. Coles, P.G. Edwards, J.S. Fleming, M.B. Hursthouse, J. Chem. Soc. Dalton Trans. (1995) 1139.
[5] (a) S.J.A. Pope, G. Reid, J. Chem. Soc. Dalton Trans. (1999) 1615. (b) J. Connolly, A.R.J. Genge, W. Levason, S.D. Orchard, S.J.A. Pope, G. Reid, J. Chem. Soc. Dalton Trans. (1999) 2343.
[6] B. Patel, S.J.A. Pope, G. Reid, Polyhedron 17 (1998) 2345.
[7] A.J. Blake, N.R. Champness, R.J. Rorder, C.S. Frampton, C.A. Frost, G. Reid, R.H. Simpson, J. Chem. Soc. Dalton Trans. (1994) 3377.
[8] R.J. Forder, G. Reid, Polyhedron 15 (1996) 3249.
[9] R.J. Forder, I.S. Mitchell, G. Reid, R.H. Simpson, Polyhedron 13 (1994) 2129.
[10] J.G. Smith, D.T. Thompson, J. Chem. Soc. A (1967) 1694. (b) P.M. Treichel, W.K. Dean, W.M. Douglas, J. Organomet. Chem. 42 (1972) 145.
[11] G.R. Willey, M.L. Butcher, M.T. Lakin, Acta Crystallogr. Sect. C 49 (1993) 1350.
[12] B.R. Kempton, W. McFarlane, A.S. Muir, P.G. Patel, J.L. Bookham, Polyhedron 12 (1993) 2525.
[13] J. Chatt, G.J. Leigh, N. Thankarayan, J. Organomet. Chem. 29 (1971) 105.
[14] P. Garrou, Chem. Rev. 81 (1981) 229.
[15] D. Rehder, in: J. Mason (Ed.), Mutinuclear NMR, Plenum Press, New York, 1987, (Chapter) 19.
[16] E.C. Alyea, R.E. Lenkinski, A. Somogyvari, Polyhedron 1 (1982) 130.
[17] F.A. Cotton, D.J. Darensbourg, S. Klein, B.W.S. Kilthammer, Inorg. Chem. 21 (1982) 2661.
[18] J.J. Eisch, R.B. King, Organomet. Synth. 1 (1965) 123.
[19] G.R. Dobson, G.C. Faber, Inorg. Chim. Acta 4 (1987) 87.

[20] G.M. Sheldrick, SHELXS86, Program for crystal structure solution, Acta Crystallogr. Sect. A 46 (1990) 467.
[21] P.T. Beurskens, G. Admiraal, G. Beurskens, W.P. Bosman, S. Garcia-Granda, R.O. Gould, J.M.M. Smits, C. Smykalla, PATTY, The DIRDIF Program System, Technical Report of the Crystallography Laboratory, University of Nijmegen, The Netherlands, 1992.
[22] TEXSAN, Crystal Structure Analysis Package, Molecular Structure Corporation, Texas, 1995.
[23] N. Walker, D. Stuart, Acta Crystallogr. Sect. A 39 (1983) 158.